

# Cholesterol accumulation and diabetes in pancreatic $\beta$ -cell-specific SREBP-2 transgenic mice: a new model for lipotoxicity

Mayumi Ishikawa,<sup>2,\*</sup> Yuko Iwasaki,<sup>2,\*</sup> Shigeru Yatoh,<sup>\*</sup> Toyonori Kato,<sup>\*</sup> Shin Kumadaki,<sup>\*</sup> Noriyuki Inoue,<sup>\*</sup> Takashi Yamamoto,<sup>\*</sup> Takashi Matsuzaka,<sup>\*,†</sup> Yoshimi Nakagawa,<sup>\*,†</sup> Naoya Yahagi,<sup>†</sup> Kazuto Kobayashi,<sup>\*</sup> Akimitsu Takahashi,<sup>\*</sup> Nobuhiro Yamada,<sup>\*</sup> and Hitoshi Shimano<sup>1,\*,†</sup>

Department of Internal Medicine (Endocrinology and Metabolism),<sup>\*</sup> Graduate School of Comprehensive Human Sciences; and Center for Advanced Research Alliance,<sup>†</sup> University of Tsukuba, 1-1-1 Tennodai, Tsukuba-City, Ibaraki, Japan, 305-8575

**Abstract** To determine the role of cholesterol synthesis in pancreatic  $\beta$ -cells, a transgenic model of *in vivo* activation of sterol-regulatory element binding protein 2 (SREBP-2) specifically in  $\beta$ -cells (TgRIP-SREBP-2) was developed and analyzed. Expression of nuclear human SREBP-2 in  $\beta$ -cells resulted in severe diabetes as evidenced by greater than 5-fold elevations in glycohemoglobin compared with C57BL/6 controls. Diabetes in TgRIP-SREBP-2 mice was primarily due to defects in glucose- and potassium-stimulated insulin secretion as determined by glucose tolerance test. Isolated islets of TgSREBP-2 mice were fewer in number, smaller, deformed, and had decreased insulin content. SREBP-2-expressing islets also contained increased esterified cholesterol and unchanged triglycerides with reduced ATP levels. Consistently, these islets exhibited elevated expression of HMG-CoA synthase and reductase and LDL receptor, with suppression of endogenous SREBPs. Genes involved in  $\beta$ -cell differentiation, such as PDX1 and BETA2, were suppressed, explaining loss of  $\beta$ -cell mass, whereas IRS2 expression was not affected. These phenotypes were dependent on the transgene expression. Taken together, these results indicate that activation of SREBP-2 in  $\beta$ -cells caused severe diabetes by loss of  $\beta$ -cell mass with accumulation of cholesterol, providing a new lipotoxic model and a potential link of disturbed cholesterol metabolism to impairment of  $\beta$ -cell function.—Ishikawa, M., Y. Iwasaki, S. Yatoh, T. Kato, S. Kumadaki, N. Inoue, T. Yamamoto, T. Matsuzaka, Y. Nakagawa, N. Yahagi, K. Kobayashi, A. Takahashi, N. Yamada, and H. Shimano. **Cholesterol accumulation and diabetes in pancreatic  $\beta$ -cell-specific SREBP-2 transgenic mice: a new model for lipotoxicity.** *J. Lipid Res.* 2008. 49: 2524–2534.

**Supplementary key words** transcription factors • sterol-regulatory element binding protein • triglycerides

This work was supported by grants-in-aid from the Ministry of Science, Education, Culture, and Technology of Japan.

Manuscript received 8 May 2008 and in revised form 15 July 2008 and in re-revised form 1 August 2008.

Published, *JLR Papers in Press*, August 8, 2008.  
DOI 10.1194/jlr.M800238-JLR200

Molecular mechanisms of pancreatic islet  $\beta$ -cell failure, a crucial pathological contributor to the development of diabetes mellitus, have been extensively explored (1). Impairment of glucose-stimulated insulin secretion (GSIS) is an early feature of type 2 diabetes. Chronic influx of FAs into  $\beta$ -cells, i.e.,  $\beta$ -cell lipotoxicity, has been thought to be involved in its pathogenesis (2).

Sterol-regulatory element binding protein 1c (SREBP-1c) is a membrane-bound transcription factor of the basic HLH (bHLH) leucine zipper family and has been established as a nutritional regulator of lipogenic enzymes in the liver (3, 4). Expression of SREBP-1c is highly upregulated by dietary intake of carbohydrates, sugars, and saturated FAs, whereas PUFAs, such as eicosapentaenoic acid, have been shown to inhibit hepatic SREBP-1c through multiple mechanisms (5, 6). These nutritional regulations of SREBP-1c are also observed in a cultured  $\beta$ -cell line and in isolated islets of mice (7, 8). SREBP-1c also plays a role in insulin signaling by inhibiting insulin receptor substrate 2 (IRS-2), the major insulin-signaling mediator in the liver and in  $\beta$ -cells (9, 10).

As a model for lipotoxicity by endogenous FAs in pancreatic  $\beta$ -cells, we previously developed transgenic mice overexpressing the active form of SREBP-1c under the insulin promoter expression (10). These mice exhibited impaired glucose tolerance *in vivo* due to both decreased  $\beta$ -cell mass and impaired insulin secretion estimated in isolated islets, which was enhanced by feeding the mice a high-fat, high-sucrose diet. The SREBP-1c-overexpressing islets had ATP depletion caused by enhanced lipogenesis and increased uncoupling protein 2 (UCP-2). Explaining the loss of  $\beta$ -cell mass, these islets had decreased expression of IRS-2 and PDX1. In addition to inhibition of GSIS,

<sup>1</sup>To whom correspondence should be addressed.  
e-mail: shimano-ty@umin.ac.jp

<sup>2</sup>M. Ishikawa and Y. Iwasaki contributed equally to this work.

SREBP-1c transgenic islets exhibited decreased potassium-stimulated insulin secretion (KSIS), which could indicate dysfunction in a process of insulin secretion following ATP production. We have recently found that granuphilin, an effector of Rab27 involving exocytosis of insulin granules, is an SREBP target and contributes at least partially to the impaired insulin secretion of islets with SREBP-1c overexpression and to diabetes (11). Conversely, islets isolated from SREBP-1-null mice exhibited increased basal insulin secretion and immunity to the impairment in insulin secretion caused by saturated FAs, establishing the contribution of SREBP-1c to lipotoxicity (7).

SREBP-2 is another member of the membrane-bound transcription factor SREBP family, and plays a crucial role in the regulation of cholesterol metabolism (12). Cellular sterol levels are controlled by feedback regulation of cholesterol biosynthetic and LDL receptor pathways. Genes in these pathways are transcriptionally regulated by SREBP-2 activation, which requires cleavage of its N-terminal bHLH portion for nuclear translocation to activate promoters of genes such as HMG-CoA reductase and synthase as well as the LDL receptor gene (13–15). FA metabolism has been well-studied with regard to its contribution to  $\beta$ -cell lipotoxicity; however, cholesterol metabolism and the role of SREBP-2 in  $\beta$ -cells have not been fully investigated. Our current study investigated whether perturbation in sterol regulation by SREBP-2 could be involved in impaired insulin secretion and  $\beta$ -cell function.

## METHODS

### Generation and maintenance of transgenic mice

The expression plasmid pRIP-SREBP-2 (1–468) containing the rat insulin I promoter (RIP; bp –715 to 31) was fused to a cDNA encoding amino acids 1–468 of human SREBP-2 (16) followed by a 3' polyadenylation signal from the human growth hormone (hGH) cDNA. Techniques used for generating transgenic mice have been described previously (17). Briefly, the *NotI-XhoI* fragment (Fig. 1A) of pRIP-SREBP-2 (1–468) was microinjected into C57BL6/J  $\times$  SJL hybrid eggs to generate transgenic mice. Founder mice were subjected to isolation of pancreatic islets, and presence of the nuclear, truncated form of human SREBP-2 was determined by RT-PCR as described below. Two independent lines of SREBP-2 transgenic mice under the control of rat insulin promoter (TgRIP-SREBP-2) were established and designated lines A and B. To obtain higher expression, hemizygotes of line A were mated to produce mice homozygous for the transgene. Mice were genotyped by PCR and Southern blot analysis. Mice were housed in colony cages and maintained on a 12 h light/12 h dark cycle. Transgenic mice and nontransgenic littermates were fed a regular chow diet (MF; Oriental Yeast, Tokyo, Japan). All experiments were performed according to the Guide for the Care and Use of Laboratory Animals at the University of Tsukuba, and the project was approved by the Institutional Review Board.

### Measurement of glucose, HbA<sub>1c</sub>, insulin, total cholesterol, triglycerides, FFA, and leptin levels

Blood was taken from the tail vein of age-matched mice fed ad libitum. The glucose level was measured with a glucose oxidase kit (Wako Pure Chemical Industries, Ltd., Osaka, Japan). The HbA<sub>1c</sub>

level was measured using an HbA<sub>1c</sub> immunoassay kit (DCA2000 system; Bayer Medical Co., Ltd., Tokyo, Japan). The insulin level was measured with a mouse insulin ELISA kit (Shibayagi Co., Ltd., Gunma, Japan). The total cholesterol, triglycerides, and FFA levels were measured with commercial kits (Wako). Leptin levels were measured with a mouse leptin ELISA kit (Morinaga Institute of Biological Science, Inc., Kanagawa, Japan).

### Glucose tolerance test

Intraperitoneal glucose tolerance test and intravenous glucose tolerance test were performed as previously described (10).

### Isolation of pancreatic islet

Mice between 16 to 24 weeks of age were used for isolation of pancreatic islets to avoid aging effects. The isolation of islets was carried out according to the Ficoll-Conray protocol (10, 18).

### Analysis of insulin secretion, insulin content, and DNA content of islets

Isolated islets were incubated for 2 h in RPMI-1640 medium supplemented with 10% FBS, 100 U/ml penicillin, and 100  $\mu$ g/ml streptomycin. Ten islets were then preincubated for 30 min in 2.8 mM glucose in 0.5% BSA Krebs-Ringer Bicarbonate Hepes (KRBH) buffer. Finally, they were incubated in 2.8 mM glucose, 20 mM glucose, or 2.8 mM glucose with 30 mM KCl in 0.5% BSA KRBH buffer for 30 min, and insulin secretion was analyzed using a mouse insulin ELISA kit (Shibayagi Co., Ltd.). Insulin and DNA content of islets were measured as described previously (10).

### Measurements of ATP and ADP of islets

ATP and ADP levels per 10 isolated islets were measured as described previously (19), using the CellTiter-Glo™ Luminescent Cell Viability Assay (Promega, Madison, WI).

### Measurements of triglycerides and cholesterol content of islets

One hundred isolated islets were used for lipid extraction. Triglycerides were measured by extracting lipids using the method of Folch, Lees, and Sloane Stanley (20), followed by triglyceride determination with the GPO-trinder kit (Sigma, St. Louis, MO). For cholesterol determination, lipids were extracted with hexane-isopropanol (3:2; v/v). The enzymatic and fluorometric method was used for the picomole determination of free and total cholesterol (21).

### Histological and immunohistochemical analysis of Islets

Mice were anesthetized, and pancreata were rapidly dissected and fixed in 4% paraformaldehyde solution, embedded in paraffin, sectioned, and stained with hematoxylin and eosin for histological analysis. For immunohistochemistry, 2  $\mu$ m sections of paraffin-embedded pancreas were dewaxed using xylene, rehydrated through serial dilutions of ethyl alcohol, and subjected to antigen retrieval using 0.1% Triton X-100 with PBS. The sections were washed and stained with the respective antibodies in staining buffer with 150 mM NaCl, 0.05% Tween-20, and 10 mM Tris-HCL (pH 7.4). Primary antibodies included guinea pig anti-insulin (DAKO Japan Co., Ltd., Kyoto, Japan) and rabbit anti-glucagon (DAKO). The secondary antibodies used included FITC-conjugated sheep anti-guinea pig IgG (P.A.R.I.S.) and Cy3-conjugated goat anti-rabbit IgG (Rockland Immunochemicals, Inc., Gilbertsville, PA).

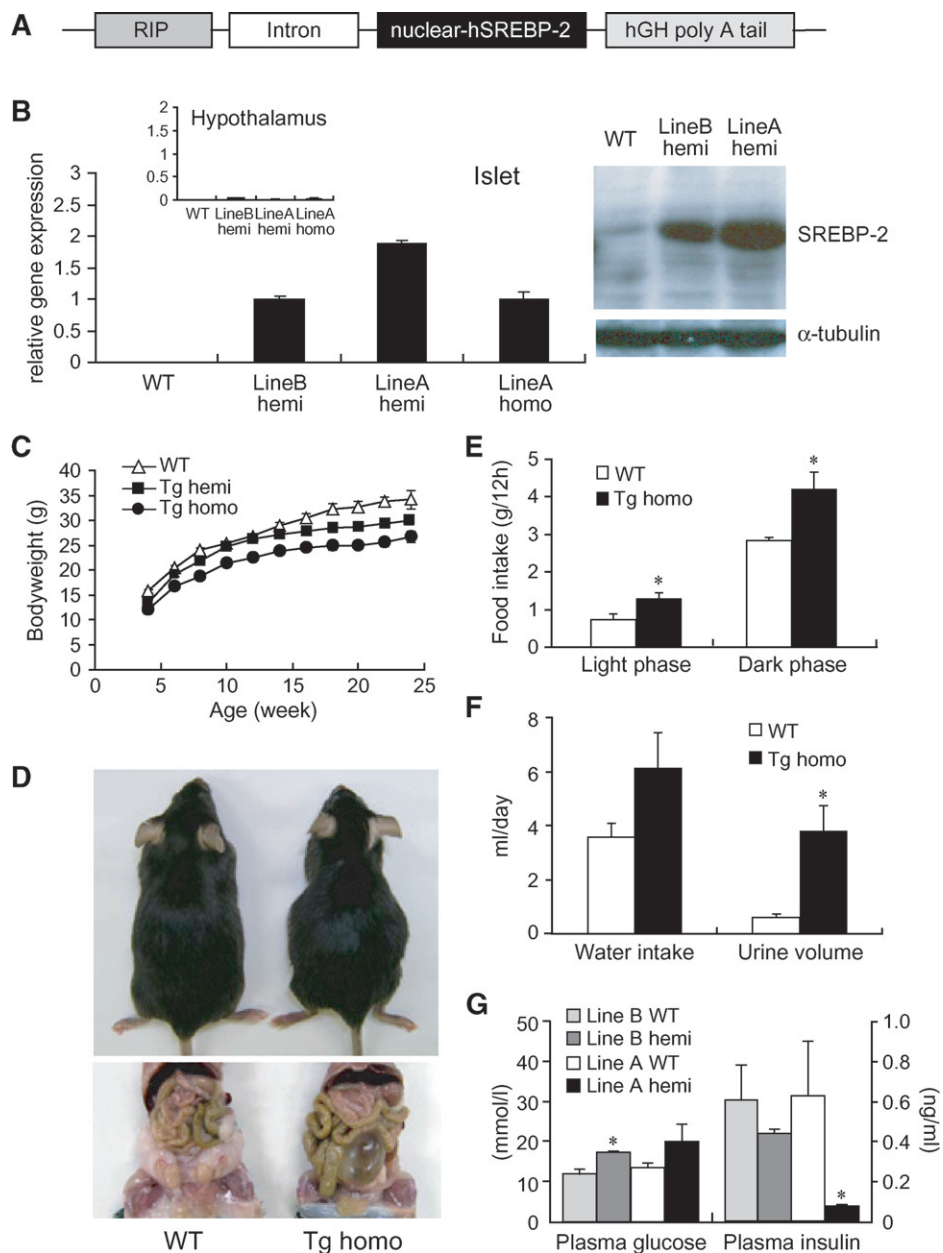


**Fig. 1.** Phenotype of sterol-regulatory element binding protein (SREBP)-2 transgenic mice expressing SREBP-2 under the control of rat insulin promoter (RIP). **A:** DNA construct for microinjection to generate Tg RIP-SREBP-2. RIP I was fused to a hybrid-adenovirus-immunoglobulin intron (Intron), and a cDNA encoding amino acids 1–468 of human SREBP-2 (nuclear-hSREBP-2) followed by a 3' polyadenylation signal from the human growth hormone cDNA (hGH poly A tail) was added. **B:** mRNA levels of the human SREBP-2 transgene in islets (left lower panel) and hypothalamus (left upper panel) from high-expression line homo (Line A homo), high-expression line hemi (Line A hemi), low-expression line hemi (Line B hemi), and wild-type (WT) littermate as estimated by real-time PCR. Results were normalized to mRNA levels of cyclophilin. Immunoblot analysis of SREBP-2 from line A hemi, line B hemi, and WT islets (right panel).  $\alpha$ -Tubulin is a loading control. **C:** Time course of body weight in male line A homo (Tg homo,  $n = 5$ ), line A hemi (Tg hemi,  $n = 8$ ), and WT ( $n = 5$ ). **D:** Appearance (top) and abdominal view (bottom) of male line A homo (Tg homo) and WT (24 weeks). **E:** Diurnal food intake was measured in 14 week-old male mice of line A homo (Tg homo,  $n = 6$ ) and WT ( $n = 6$ ).  $*P < 0.05$ , compared with WT. **F:** Twenty-four hour water intake and urine volume in 12 week-old male mice of line A homo (Tg homo,  $n = 5$ ) and WT ( $n = 5$ ) were measured in individually housed mice.  $*P < 0.05$ , compared with WT. **G:** Intraperitoneal glucose tolerance tests in 8 week-old male mice. Plasma glucose and plasma insulin levels of line A hemi, line A WT, line B hemi, and line B WT ( $n = 4$  for each group) were measured 15 min after intraperitoneal injection of glucose (1 g/kg body weight) following an overnight fast.  $*P < 0.05$ , compared with WT of each group.

## Preparation of islet RNA and estimation of gene expression

Total RNA extraction with the TRIzol reagent (Invitrogen, Carlsbad, CA) and DNase-I treatment using the RNeasy Micro Kit (Qiagen, Hilden, Germany) were performed according to the manufacturers' instructions. Northern blot analysis was performed with the indicated cDNA probes using Rapid-hyb buffer (GE Healthcare UK, Ltd.). cDNA was synthesized with the ThermoScript™RT-PCR system (Invitrogen) and real-time fluorescent detection PCR analysis was performed using Sybr-Green Dye (ABgene, UK) with an ABI 7000 PCR instrument (Applied Biosystems Japan, Ltd., Tokyo, Japan) as previously described (11). mRNA level was normalized to cyclophilin expression.

## Immunoblot analysis

Islets were harvested and dissolved in lysis buffer containing 20 mM Hepes (pH 7.6), 150 mM NaCl, 1% NP-40, 0.5% sodium deoxycholate, 0.1% SDS, 10% glycerol, 25 µg/ml calpain inhibitor, 10 µg/ml aprotinin, and 10 µg/ml leupeptin. Immunoblot analysis was as previously described (10). Cell extracts from isolated islets were probed with polyclonal antibodies against SREBP-2 (K0180-3; Medical and Biological Laboratories Co., Ltd, Nagoya, Japan), PDX1 (#07-696; Upstate), α-tubulin (sc-5286; Santa Cruz Biotechnology, Santa Cruz, CA), and Lamin A/C (#2032; Cell Signaling). Detection was performed using an ECL advance Western blotting detection kit and Hyperfilm ECL (GE Healthcare).

## Expression plasmid and reporter plasmids

For generation of a human nuclear SREBP-2 expression plasmid, the same cDNA fragment used for producing TgRIP-SREBP-2 constructs was cloned into cDNA3.1(+) (Invitrogen). RIP-luciferase reporter plasmid and sterol-regulatory element (SRE)-luciferase reporter plasmid were produced as previously described (22, 23).

## Cell culture, transfection, and luciferase assays

MIN6 cells were maintained in DMEM containing 25 mmol/l glucose supplemented with 15% FBS, β-mercaptoethanol (5 µl/l), penicillin (100 U/ml), and streptomycin (100 µg/ml) at 37°C in an atmosphere of 95% air/5% CO<sub>2</sub>. The cells were seeded onto 24-well plates at a density of 3 × 10<sup>5</sup> cells/ml and cultured overnight to 80% confluency. The cells were transfected with an RIP-luciferase reporter plasmid or SRE-luciferase reporter plasmid, and an expression vector for nuclear SREBP-2 using Lipofectamine 2000 reagent (Invitrogen) according to the manufacturer's instructions. Total amount of plasmid DNA was always 300 ng/ml. After a 48 h incubation, the amount of firefly luciferase activity in transfectants was measured.

## Statistical analysis

Data are expressed as the mean ± standard error of the mean (SEM) except for the data of the estimation of gene expression and the luciferase assays that were expressed as the mean ± standard deviation (SD).

## RESULTS

### Phenotypic features of TgRIP-SREBP-2 mice

Transgenic mice overexpressing the nuclear form of human SREBP-2 under control of the RIP I (TgRIP-SREBP-2) were created (Fig. 1A). Specificity of transgene expression was verified by RT-PCR to demonstrate that human SREBP-2 was expressed in pancreatic islets (Fig. 1B, left). The

TABLE 1. Body weights and organ weights in 24 week-old mice

	WT	Tg Hemi	Tg Homo
Body weight (g)	35.9 ± 3.5	29.8 ± 0.7	28.6 ± 0.7
Liver (% BW)	5.1 ± 0.8	6.0 ± 0.5	6.2 ± 0.2
Kidney (% BW)	1.0 ± 0.1	1.5 ± 0.1	1.9 ± 0.1 <sup>a</sup>
White adipose tissue (% BW)	3.6 ± 0.9	1.6 ± 0.4 <sup>a</sup>	0.4 ± 0.4 <sup>a</sup>

WT, wild type; BW, body weight; Tg, transgenic; TgRIP-SREBP-2 mice of high-expression line (line A, n = 4 for each group) were sacrificed in a fed condition. Data represent means ± SEM.

<sup>a</sup> P < 0.05, compared with WT.

transgene caused a robust increase in SREBP-2 protein in islets as estimated by immunoblot analysis (Fig. 1B, right). A high expressor, line A, and a low expressor, line B, were established based upon consistent increases in both mRNA and protein levels of human SREBP-2 in islets. Leaky gene expression from the RIP promoter is often noted, however. SREBP-2 in the hypothalamus was essentially negative in both lines (Fig. 1B, inset). In addition, there was no change in hypothalamic expression of HMG-CoA synthase, an SREBP-2 target gene (data not shown). Line A transgenic

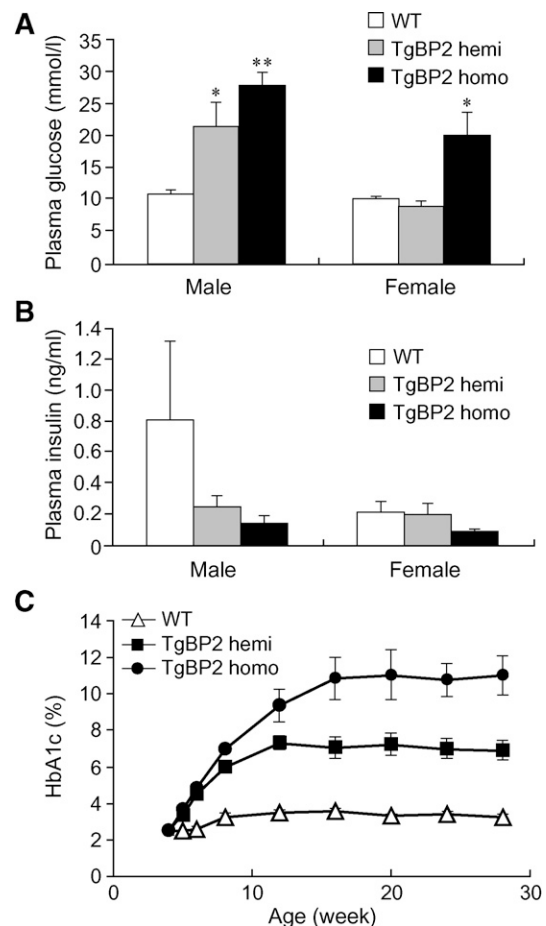
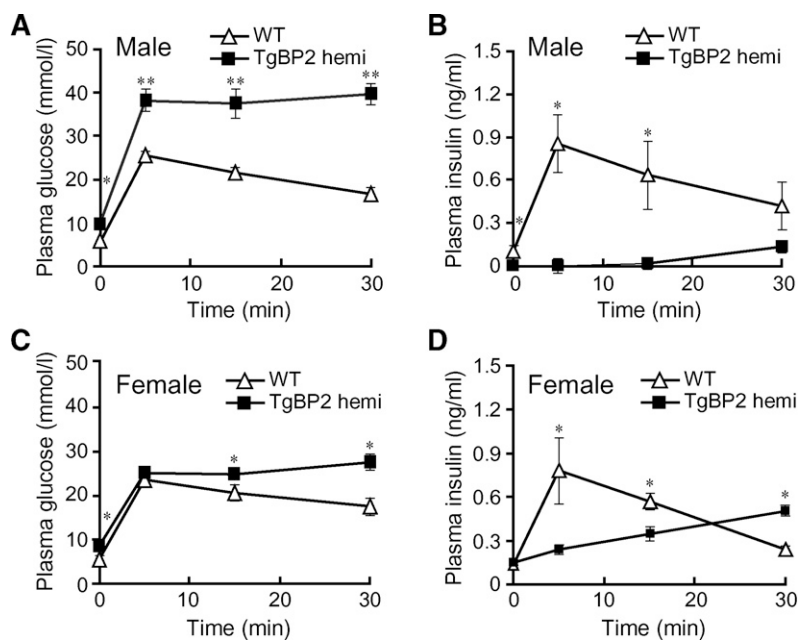


Fig. 2. Plasma glucose, insulin, and HbA<sub>1c</sub> levels of TgRIP-SREBP-2 mice. A: Plasma glucose levels of line A homo (TgBP2 homo), line A hemi (TgBP2 hemi), and WT (n = 4–6). \*P < 0.05 and \*\*P < 0.01, compared with WT of each group. B: Plasma insulin levels of line A homo (TgBP2 homo), line A hemi (TgBP2 hemi), and WT (n = 4–6). C: Time course of HbA<sub>1c</sub> levels in male line A homo (TgBP2 homo), line A hemi (TgBP2 hemi), and WT (n = 6–10).



**Fig. 3.** Intravenous glucose tolerance tests in TgRIP-SREBP-2 mice. Plasma glucose and plasma insulin levels of 8 week-old mice were measured after intravenous injection of glucose (1 g/kg body weight) following an overnight fast. A: Plasma glucose levels of male line A hemi (TgBP2 hemi,  $n = 5$ ) and WT ( $n = 5$ ) mice. B: Plasma insulin levels of male line A hemi (TgBP2 hemi,  $n = 5$ ) and WT ( $n = 5$ ) mice. C: Plasma glucose levels of female line A hemi (TgBP2 hemi,  $n = 5$ ) and WT ( $n = 5$ ) mice. D: Plasma insulin levels of female line A hemi (TgBP2 hemi,  $n = 5$ ) and WT ( $n = 5$ ) mice. \* $P < 0.05$  and \*\* $P < 0.01$ , compared with WT of each group.

hemizygous mice (hereafter referred to as TgRIP-SREBP-2 hemi) were used to produce mice homozygous for the transgene (hereafter referred to as TgRIP-SREBP-2 homo) for further studies. Growth curve was slightly retarded in TgRIP-SREBP-2 homo mice as compared with wild-type control littermates (Fig. 1C). Gross appearance of TgRIP-SREBP-2 homo mice was characterized by a thinner body with a distended flank (Fig. 1D, upper panel), which was caused by enlarged urine-filled bladder as was apparent upon anatomical inspection (Fig. 1D, lower panel). Adipose tissue mass was markedly diminished, explaining the body weight loss, whereas kidneys were enlarged (Table 1). Body length was not changed. TgRIP-SREBP-2 homo mice exhibited increased food intake, water intake, and urine volume compared with controls (Fig. 1E, F).

#### Insulin-deficient diabetes in TgRIP-SREBP-2

Consistent with these typical signs of diabetes (polyuria, polydipsia, and hyperphagia), TgRIP-SREBP-2 mice (line A) were diabetic, with homo more severe. Hemizygotes of line B (low expressors) were not diabetic, but still exhibited impaired plasma insulin and higher glucose levels based on intraperitoneal glucose tolerance tests (Figs. 1G, 2). In both TgRIP-SREBP-2 hemi and TgRIP-SREBP-2 homo mice from line A, plasma glucose was markedly increased,

whereas plasma insulin was diminished (Fig. 2A, B). Glycohemoglobin, as a chronic marker for hyperglycemia, was steadily increased up to 16 weeks, and sustained at the high levels of 7% and 11% in TgRIP-SREBP-2 hemi and homo mice, respectively (Fig. 2C). Thus, these diabetic signs and symptoms depended upon the expression of the SREBP-2 transgene. Intravenous glucose tolerance tests on TgRIP-SREBP-2 hemi mice showed extended hyperglycemia and markedly impaired insulin levels after glucose loading as compared with wild-type mice (Fig. 3). The diabetes in the transgenic mice was milder in females than in males.

Plasma lipids in TgRIP-SREBP-2 homo were changed consistent with the pattern seen in insulin-depleted diabetic patients, often referred to as diabetic lipemia, i.e., increased plasma triglycerides and FFAs and no marked change in cholesterol (Table 2). Plasma leptin levels were dramatically decreased, reflecting emaciation in TgRIP-SREBP-2 homo mice (control:  $14.5 \pm 4.0$  ng/ml vs. TgBP2 homo  $1.5 \pm 0.5$  ng/ml,  $n = 5$ ).

#### Characterization of pancreatic islets from TgRIP-SREBP-2 mice

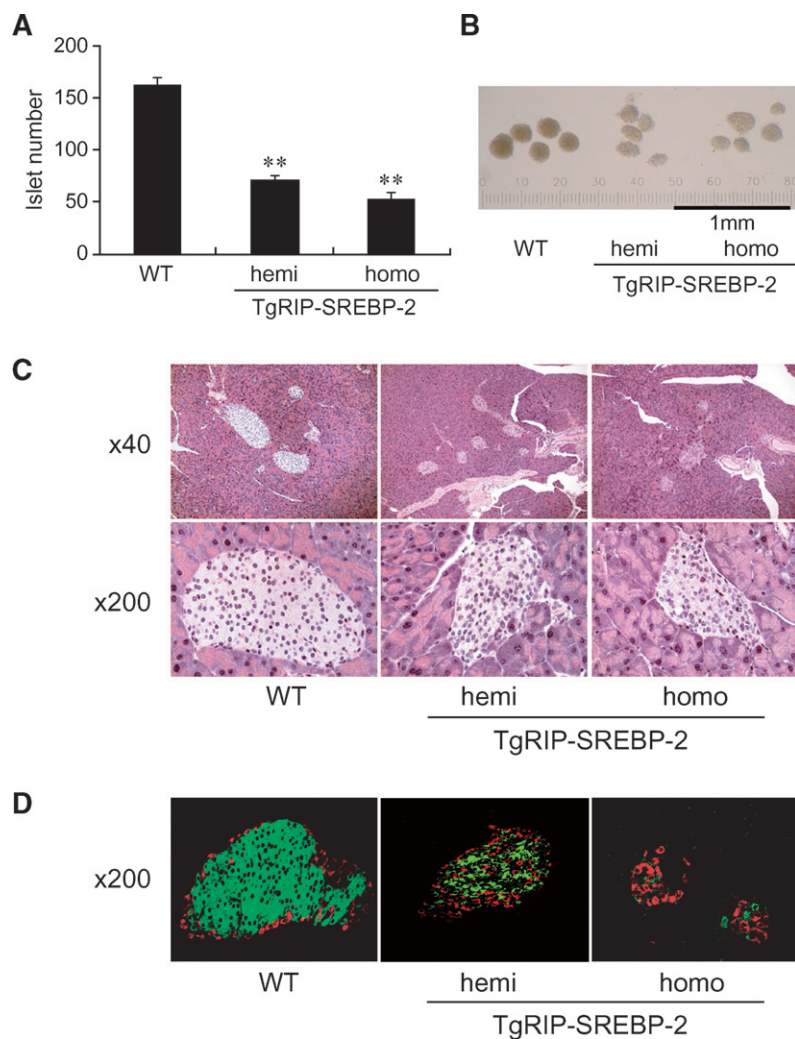
Pancreatic islets from TgRIP-SREBP-2 hemi and TgRIP-SREBP-2 homo mice were isolated and morphologically compared with islets from wild-type control animals (Fig. 4).

TABLE 2. Plasma parameters in 12 week-old mice

	Male			Female		
	WT	Tg Hemi	Tg Homo	WT	Tg Hemi	Tg Homo
TC (mg/dl)	$87.9 \pm 6.8$	$87.8 \pm 6.8$	$87.5 \pm 19.6$	$67.2 \pm 2.5$	$72.8 \pm 2.2$	$61.6 \pm 6.5$
TG (mg/dl)	$73.5 \pm 13.1$	$82.6 \pm 8.2$	$129.3 \pm 54.7$	$39.9 \pm 1.8$	$38.0 \pm 2.7$	$85.0 \pm 15.4$
FFA (mEq/l)	$0.53 \pm 0.04$	$0.54 \pm 0.11$	$0.97 \pm 0.28$	$0.49 \pm 0.06$	$0.60 \pm 0.05$	$0.96 \pm 0.18^a$

TG, triglyceride; TC, total cholesterol; The blood of TgRIP-SREBP-2 mice of high-expression line (line A,  $n = 5$  for each group) was drawn in fed condition. Data represent means  $\pm$  SEM.

<sup>a</sup>  $P < 0.05$ , compared with WT.



**Fig. 4.** Isolated islet number and morphology of pancreas sections from TgRIP-SREBP-2 mice. **A:** Pancreatic islets were isolated from male mice of line A homo (homo), line A hemi (hemi), and WT ( $n = 8-10$ ) age 16 to 24 weeks and counted manually.  $**P < 0.01$ , compared with WT. **B:** Representative isolated islets were photographed through stereomicroscopy. **C:** Representative pancreas sections of line A homo, line A hemi, and WT were stained with hematoxylin and eosin for histological analysis. Original magnification,  $\times 40$  (top panels);  $\times 200$  (bottom panels). **D:** Representative islets from pancreas sections of line A homo (homo), line A hemi (hemi), and WT stained with immunofluorescent antibodies for insulin (green) and glucagon (red) as described in the Methods section. Original magnification,  $\times 200$ .

The number and size of islets from the transgenic mice were both decreased (Fig. 4A, B). Islets from TgRIP-SREBP-2 mice did not display the typical rounded shape of a normal islet, and the color was changed from dark to pale brown, presumably due to reduced cellularity in TgRIP-SREBP-2 islets, which was more prominent in homozygote compared with hemizygote mice (Fig. 4B). Histological section demonstrated that smaller and deformed islets of TgRIP-SREBP-2 mice were located close to connective tissues containing pancreatic ducts (Fig. 4C). Immunological staining showed that insulin immunoreactivity was diminished and scattered, whereas peripheral staining of glucagon observed in a normal islet was altered to a scattered pattern (Fig. 4D). These changes in the pattern of  $\alpha$ - and  $\beta$ -cells were more severe in homozygotes than in hemizygotes. These data indicate that islets of TgRIP-SREBP-2 mice were structurally abnormal and had less  $\beta$ -cells and insulin content.

#### Impaired insulin secretion from TgRIP-SREBP-2 islets

Isolated islets were tested for insulin secretion (Fig. 5). Basal (low glucose), glucose-stimulated, and KSIS were severely impaired in both TgRIP-SREBP-2 homo and TgRIP-SREBP-2 hemi mice when determined on the basis of islet

number (Fig. 5A). Other insulin secretagogues, such as GLP-1 and glibenclamide, also failed to enhance insulin secretion in TgRIP-SREBP-2 hemi islets (Fig. 5B). DNA and insulin content per islet were slightly and severely suppressed, respectively. Thus, when normalized to insulin content, impaired insulin secretion was obscured in TgRIP-SREBP-2 islets (Fig. 5C, D). Both ATP and ADP contents were also decreased (Fig. 5E).

To estimate the consequences of nuclear SREBP-2-activated lipid synthesis, lipid content in islets was measured (Fig. 6). TgRIP-SREBP-2 hemi islets from line A exhibited significant increases in cholesteryl ester (Fig. 6A), whereas triglyceride content was not changed (Fig. 6B). It was in good contrast to TgRIP-SREBP-1c islets that exhibited increases in triglycerides but not in cholesterol (Fig. 6B) (10). Hemizygous mice from the low expressor, line B, showed no significant increases in islet cholesterol or triglyceride content. Gene expression of the islets was examined. Cholesterol biosynthetic genes, HMG-CoA synthase and reductase, and LDL receptor are major targets of SREBP-2 and were consistently elevated in TgRIP-SREBP-2 homo islets (Fig. 7A). TgRIP-SREBP-2 hemi islets also exhibited an increasing trend in expression of SREBP-2 target genes, with the exception of HMG-CoA synthase. As shown in

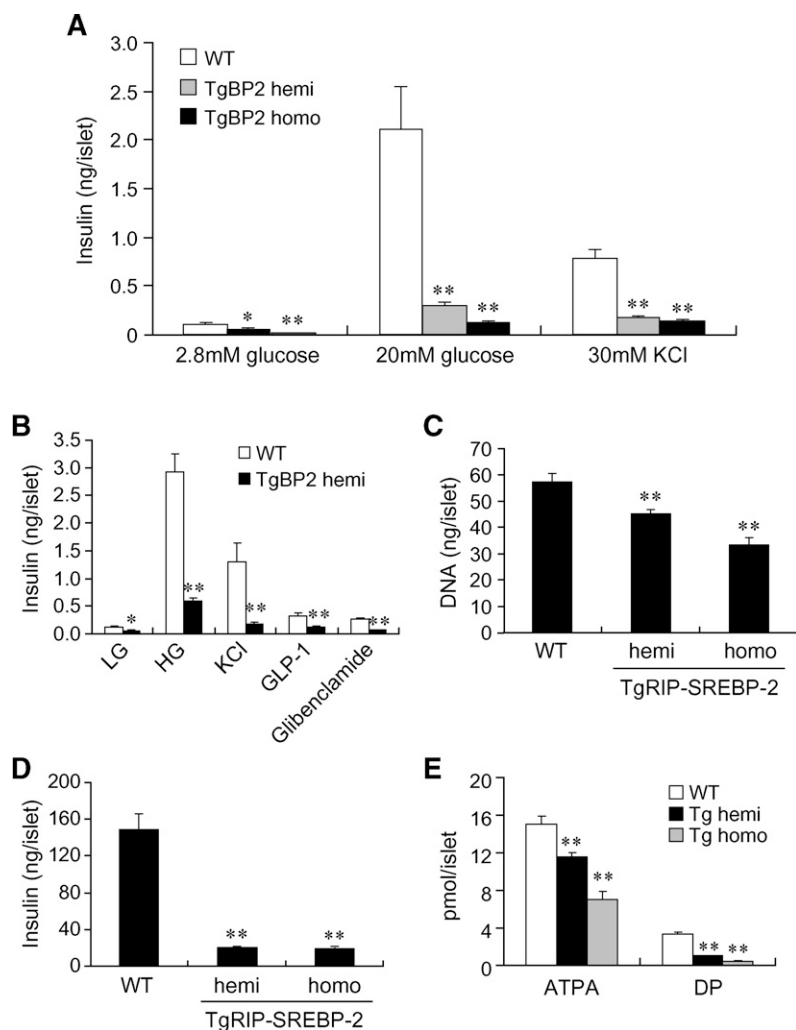


**Fig. 5.** Insulin content and ATP/ADP levels in islets from TgRIP-SREBP-2 mice. **A:** Insulin secretion from isolated islets of line A homo (TgBP2 homo), line A hemi (TgBP2 hemi), and WT. Ten islets of similar size from each group (6–10 batches) were incubated in 0.5% BSA KRBH buffer containing 2.8 mM glucose, 20 mM glucose, or 2.8 mM glucose with 30 mM KCl, and insulin secretion per islet was measured. **B:** Stimulation of insulin secretion by GLP-1 (100 nM) or glibenclamide (0.3 mM) from isolated islet of line A hemi (TgBP2 hemi) and WT. **C:** DNA content per islet from line A homo (homo), line A hemi (hemi), and WT (7–11 batches). **D:** Insulin content per islet from line A homo (homo), line A hemi (hemi), and WT (8–12 batches). **E:** ATP and ADP levels per islet from line A homo (TgBP2 homo), line A hemi (TgBP2 hemi), and WT (8–12 batches). \* $P < 0.05$  and \*\* $P < 0.01$ , compared with WT of each group.

Fig. 7B, SREBP-2 overexpression also increased FA synthase gene expression. Endogenous SREBP-1 and -2 genes were downregulated. Liver X receptor (LXR)- $\alpha$ , but not - $\beta$  was increased; however, ABCA-1 and ABCG-1, targets of LXRs, were decreased in TgRIP-SREBP-2 homo islets. These results suggest that unregulated activation of cholesterologenic genes caused by SREBP-2 overexpression in islets of TgRIP-SREBP-2 was still sustained despite over-accumulation of cholesterol.  $\beta$ -cell-specific transcription factors PDX1 and BETA2/NeuroD were suppressed, whereas neurogenin 3 (ngn3) was upregulated (Fig. 8A). PDX1 protein was also decreased in SREBP-2 overexpression (Fig. 8B). Unlike TgRIP-SREBP-1c islets and SREBP-1 overexpressing livers (9, 10), IRS-2 was not decreased in TgRIP-SREBP-2 islets. Granuphilin, a recently identified SREBP-1 target gene involved in insulin secretion impairment (11), was not significantly changed in TgRIP-SREBP-2 islets. Suppression of PDX1 and BETA2 could explain deformed shape and altered components of insulin and glucagon-staining cells in pancreatic islets of aged TgRIP-SREBP-2 mice. These abnormal structures of islets were already observed in TgRIP-SREBP-2 mice by the age of 2 weeks (Fig. 8B), indicating that impairment of  $\beta$ -cell differentiation was a primary event, and not secondary to the emergence of diabetes in

TgRIP-SREBP-2 mice. Insulin mRNA was also decreased in TgRIP-SREBP-2 hemi islets from line A (Fig. 8C). Downregulation of insulin expression could be due at least partially to inhibition of transcription by overexpression of nuclear SREBP-2, because the insulin promoter was downregulated by overexpression of SREBP-2 in a luciferase reporter assay in MIN6 cells (Fig. 8E).

## DISCUSSION

Our current studies clearly demonstrated that chronic activation of SREBP-2 in  $\beta$ -cells caused severe diabetes with insulin depletion. The insulin depletion in vivo was due to both reduction of  $\beta$ -cell mass and impaired insulin secretion per islet as observed in high expressor (line A) and low expressor (line B), respectively. Comparing the severity of diabetes among homo and hemi line A and line B mice, decreased  $\beta$ -cell mass is probably the major cause of diabetes in line A. Overall, the severity of the phenotype, including hyperglycemia, insulin secretion defect, and islet mass loss, were dependent on the transgene expression level.

The islets and  $\beta$ -cells from TgRIP-SREBP-2 mice were abnormal in many different ways. Islet mass reduction

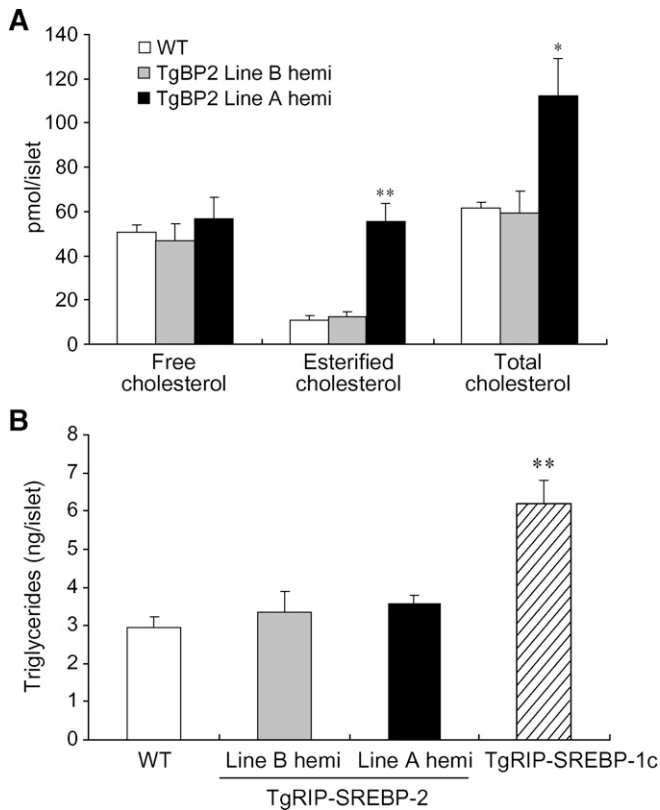


**Fig. 6.** Lipid content in isolated islets from TgRIP-SREBP-2 mice. **A:** Cholesteryl ester and free cholesterol of 100 islets isolated from high expression line hemi (TgBP2 Line A hemi), low expression line hemi (TgBP2 Line B hemi), and WT (6–8 batches) were extracted and measured as described in the Methods section. **B:** Triglycerides of 100 islets isolated from high-expression line A hemi (Line A hemi), low-expression line B hemi (Line B hemi), WT, and  $\beta$ -cell-specific nuclear SREBP-1c transgenic mice (TgRIP-SREBP-1c) were extracted and measured as described in the Methods section (5 batches for each group). \* $P < 0.05$  and \*\* $P < 0.01$ , compared with WT of each group.

was characterized by decreased islet number, decreased  $\beta$ -cell number per islet, and decreased insulin content per islet. The smaller and deformed islets were connected to or located close to connective tissues surrounding pancreatic ducts. These changes in islet construction were similar to those noted in PDX1 and IRS-1 double heterozygote knockout mice, or E2F1 knockout mice (24–26). Expression of PDX1 and BETA2 was suppressed in islets of TgRIP-SREBP-2. Because both transcription factors are intimately involved in islet genesis, especially  $\beta$ -cell genesis (27–29), suppression of these factors could explain the  $\beta$ -cell mass reduction that was observed even at an early age in these mice. Mice with heterozygous PDX1 gene disruption have been reported to exhibit enhanced  $\beta$ -cell apoptosis (30), but apoptosis of  $\beta$ -cells was barely observed in both TgRIP-SREBP-2 and control islets assessed by TUNEL staining (data not shown). These data suggest that  $\beta$ -cell reduction was due mainly to impaired  $\beta$ -cell genesis. Our preliminary data indicate that repression of PDX1 and BETA2, as well as the insulin gene, by SREBP-2 could be mediated by inhibiting promoters of these genes

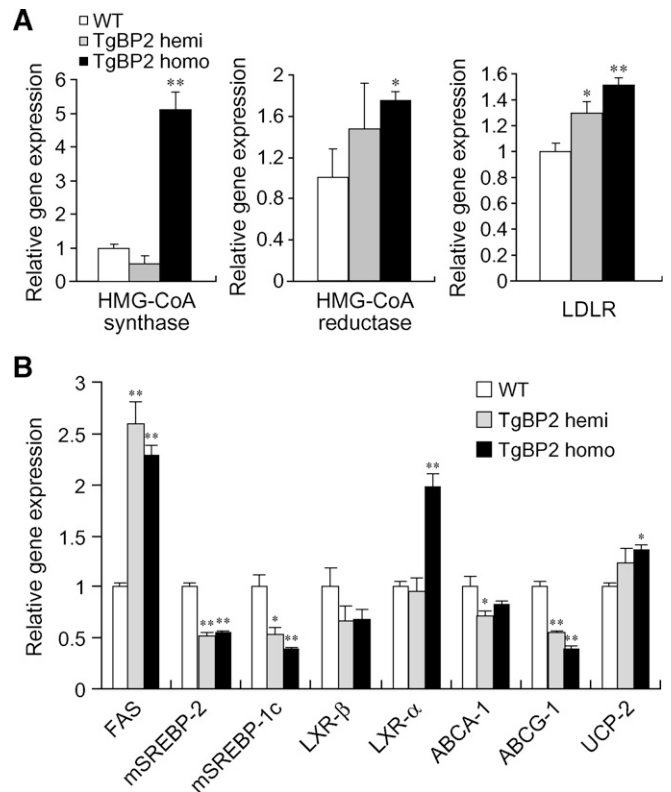


**Fig. 7.** Expression of cholesterol-related genes in isolated islets from TgRIP-SREBP-2 mice. **A:** mRNA levels of HMG-CoA synthase, HMG-CoA reductase, and LDL receptor (LDLR) in islets from line A homo (TgBP2 homo), line A hemi (TgBP2 hemi), and WT. **B:** mRNA levels of FA synthase (FAS), endogenous SREBPs, liver X receptor (LXR)- $\beta$  and - $\alpha$ , ABCA-1, ABCG-1, and uncoupling protein 2 (UCP-2) in islets from line A homo (TgBP2 homo), line A hemi (TgBP2 hemi), and WT. All results were normalized to mRNA levels of cyclophilin. Experiments were performed in triplicate wells on sets of islets from three to six mice per replicate. \* $P < 0.05$  and \*\* $P < 0.01$ , compared with WT of each group.

(Fig. 8D, E). The precise molecular mechanism is currently under investigation.

TgRIP-SREBP-2 mice accumulate only cholesteryl esters and not triglycerides in the islets, contrasting with islets from TgRIP-SREBP-1c mice, which exhibit accumulation of triglycerides but not cholesteryl esters. Consistently, TgRIP-SREBP-1c islets induced genes for FA synthesis and not genes for cholesterol synthesis, whereas elevation of gene expression of cholesterogenic genes and LDL receptor gene were prominent in TgRIP-SREBP-2 mice. In addition to this distinction in lipid synthesis, the expression pattern of genes known to affect  $\beta$ -cell function was different between mice expressing islet-specific SREBP-1c and those expressing SREBP-2. IRS-2, reported to be important for growth and survival of  $\beta$ -cells via insulin signaling (31–33), was decreased in islets of TgRIP-SREBP-1c mice, partially contributing to the decreased  $\beta$ -cell mass, especially when mice were fed a high-fat diet. In contrast, IRS-2 expression was sustained in TgRIP-SREBP-2  $\beta$ -cells. Similarly, UCP-2, an important contributor to lipotoxicity (34–37) was markedly upregulated in TgRIP-SREBP-1c islets



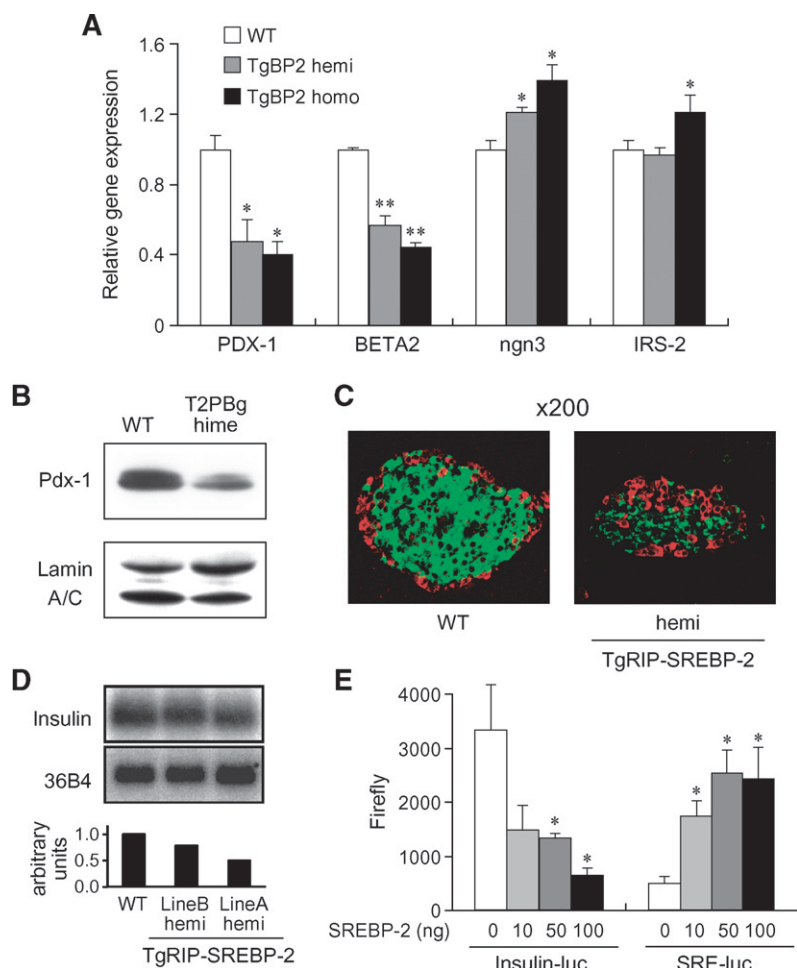



**Fig. 8.**  $\beta$ -Cell-specific factors and insulin in isolated islets from TgRIP-SREBP-2 mice. **A:** mRNA levels of PDX1, BETA2/NeuroD, neurogenin3 (ngn3), and insulin receptor substrate 2 (IRS-2) in isolated islets from line A homo (TgBP2 homo), line A hemi (TgBP2 hemi), and WT mice, age 16 to 24 weeks, by real-time PCR. All results were normalized to mRNA levels of cyclophilin. Experiments were performed in triplicate wells on sets of islets from three to six mice per replicate. \* $P < 0.05$  and \*\* $P < 0.01$ , compared with WT of each group. **B:** PDX1 protein in islets of TgRIP-SREBP-2 (line A hemi) mice with Lamin A/C as a loading control as estimated by immunoblot analysis. **C:** Formation of islets during differentiation of  $\beta$ -cell in TgRIP-SREBP-2 mice. Representative islets from pancreas sections of line A hemi (TgBP2 hemi) and WT at the age of 2 weeks stained with immunofluorescent antibodies for insulin (green) and glucagon (red) as described in the Methods section. Original magnification,  $\times 200$ . **D:** Insulin gene expression and its quantification in isolated islets from high-expression line hemi (Line A hemi), low-expression line hemi (Line B hemi), and WT as estimated by Northern blot analysis. **E:** Activation of the insulin gene promoter by SREBP-2 in MIN6 cells. MIN6 cells were transfected with an RIP-luciferase reporter plasmid (Insulin-luc) or an SRE-luciferase reporter plasmid (SRE-luc), and 0, 10, 50, 100 ng of expression vector for nuclear SREBP-2 (SREBP-2) for 48 h. The cells were subjected to reporter assays for measurement of firefly luciferase activity. Experiments were performed in triplicate. \* $P < 0.05$ , compared with control (SREBP-2 expression vector = 0 ng) for each group.

(10), whereas it was increased only slightly in TgRIP-SREBP-2 islets. These data indicate that the mechanism for decreased  $\beta$ -cell mass was not identical between SREBP-2 and SREBP-1c transgenic mice. Downregulation of IRS-2 and upregulation of UCP-2 were observed in islets of diet-induced obese mice and isolated islets treated with saturated FAs. This is consistent with the fact that TgRIP-SREBP-1c mice required consumption of a high-fat diet to induce diabetes. Thus, IRS-2 and UCP-2 are FA-related mediators of  $\beta$ -cell lipotoxicity, but are not involved in the development of diabetes caused by islet SREBP-2 overexpression.  $\beta$ -cell failure and diabetes were more severe in TgRIP-SREBP-2 than in TgRIP-SREBP-1c mice, although a precise comparison of nuclear protein level or stoichiometric estimation has not been performed. It is currently unknown whether this is due to potential toxicity of cholesterol accumulation or whether there are other genes specific to SREBP-2 and not SREBP-1 that cause  $\beta$ -cell failure (such as PDX1 and BETA2), or both.

One important aspect of this study is the potential effect of disturbed cholesterol metabolism on  $\beta$ -cell function. Accumulation of cholesterol could be a cellular stress or could be toxic, and lead to  $\beta$ -cell failure through a different mechanism than accumulation of triglycerides as was observed in TgRIP-SREBP-1c and other lipotoxic models (38). Accumulation of cholesterol could also contribute

to loss of  $\beta$ -cell mass. It has been recently reported that treatment with a high dose of statins, inhibitors of HMG-CoA reductase, caused disturbed insulin secretion in a  $\beta$ -cell line (39), indicating that disturbed cholesterol metabolism could affect insulin secretion. Inhibition of cholesterol synthesis by HMG-CoA reductase inhibitors caused initial intracellular cholesterol depletion, but secondarily, adaptive SREBP-2 activation, as was induced in vivo in our current study. Our data imply that in addition to well-established FAs, cholesterol could be added to the list of lipotoxic agents and that SREBP-2, a key transcription factor for cholesterol synthesis, could be a direct and/or indirect mediator of this new type of lipotoxicity. A recent paper reported, from studies on ABCA-1-null mice, that ABCA-1, a cellular cholesterol transporter, was shown to regulate cholesterol homeostasis and insulin secretion in pancreatic  $\beta$ -cells (40, 41). Their data and our current data consistently demonstrate that alterations of islet cholesterol levels through cholesterol efflux and cholesterol synthesis, respectively, could contribute to islet dysfunction and loss of insulin secretion. In addition, a direct link between elevated serum cholesterol and reduced insulin secretion has been reported (42). Using a combination of apolipoprotein E knockout and ob/ob mice, they showed a correlation between islet cholesterol content and impaired GSIS. The impaired GSIS was restored by

cholesterol depletion with T $\beta$ CD or statin. We also observed increased cholesterol content in islets of db/db mice (data not shown). In contrast to the pathological process caused by elevated plasma cholesterol level, our model also implies that endogenous cholesterol accumulation could lead to  $\beta$ -cell dysfunction.

Collectively, current data indicate that chronic activation of SREBP-2 impairs  $\beta$ -cell mass and function through its own transcription effect and cholesterol accumulation. Elucidation of the clinical relevance of this artificial system to human diabetes requires precise estimation of nuclear SREBP-2 protein in  $\beta$ -cells from patients with diabetes. Further studies are needed to clarify the details and the precise mechanisms of a link between cholesterol metabolism and insulin secretion. 

The authors are grateful to Dr. Alyssa H. Hasty for careful reading of this manuscript.

## REFERENCES

- Kahn, S. E. 2003. The relative contributions of insulin resistance and beta-cell dysfunction to the pathophysiology of Type 2 diabetes. *Diabetologia*. **46**: 3–19.
- Unger, R. H. 1995. Lipotoxicity in the pathogenesis of obesity-dependent NIDDM. Genetic and clinical implications. *Diabetes*. **44**: 863–870.
- Shimano, H., N. Yahagi, M. Amemiya-Kudo, A. H. Hasty, J. Osuga, Y. Tamura, F. Shionoiri, Y. Iizuka, K. Ohashi, K. Harada, et al. 1999. Sterol regulatory element-binding protein-1 as a key transcription factor for nutritional induction of lipogenic enzyme genes. *J. Biol. Chem.* **274**: 35832–35839.
- Shimano, H. 2002. Sterol regulatory element-binding protein family as global regulators of lipid synthetic genes in energy metabolism. *Vitam. Horm.* **65**: 167–194.
- Horton, J. D., Y. Bashmakov, I. Shimomura, and H. Shimano. 1998. Regulation of sterol regulatory element binding proteins in livers of fasted and re-fed mice. *Proc. Natl. Acad. Sci. USA*. **95**: 5987–5992.
- Yahagi, N., H. Shimano, A. H. Hasty, M. Amemiya-Kudo, H. Okazaki, Y. Tamura, Y. Iizuka, F. Shionoiri, K. Ohashi, J. Osuga, et al. 1999. A crucial role of sterol regulatory element-binding protein-1 in the regulation of lipogenic gene expression by polyunsaturated fatty acids. *J. Biol. Chem.* **274**: 35840–35844.
- Kato, T., H. Shimano, T. Yamamoto, M. Ishikawa, S. Kumadaki, T. Matsuzaka, Y. Nakagawa, N. Yahagi, M. Nakakuki, A. H. Hasty, et al. 2008. Palmitate impairs and eicosapentaenoate restores insulin secretion through regulation of SREBP-1c in pancreatic islets. *Diabetes*. **57**: 2382–2392.
- Shimano, H., M. Amemiya-Kudo, A. Takahashi, T. Kato, M. Ishikawa, and N. Yamada. 2007. Sterol regulatory element-binding protein-1c and pancreatic beta-cell dysfunction. *Diabetes Obes. Metab.* **9** (Suppl.): 133–139.
- Ide, T., H. Shimano, N. Yahagi, T. Matsuzaka, M. Nakakuki, T. Yamamoto, Y. Nakagawa, A. Takahashi, H. Suzuki, H. Sone, et al. 2004. SREBPs suppress IRS-2-mediated insulin signalling in the liver. *Nat. Cell Biol.* **6**: 351–357.
- Takahashi, A., K. Motomura, T. Kato, T. Yoshikawa, Y. Nakagawa, N. Yahagi, H. Sone, H. Suzuki, H. Toyoshima, N. Yamada, et al. 2005. Transgenic mice overexpressing nuclear SREBP-1c in pancreatic beta-cells. *Diabetes*. **54**: 492–499.
- Kato, T., H. Shimano, T. Yamamoto, T. Yokoo, Y. Endo, M. Ishikawa, T. Matsuzaka, Y. Nakagawa, S. Kumadaki, N. Yahagi, et al. 2006. Granuphilin is activated by SREBP-1c and involved in impaired insulin secretion in diabetic mice. *Cell Metab.* **4**: 143–154.
- Horton, J. D., I. Shimomura, M. S. Brown, R. E. Hammer, J. L. Goldstein, and H. Shimano. 1998. Activation of cholesterol synthesis in preference to fatty acid synthesis in liver and adipose tissue of transgenic mice overproducing sterol regulatory element-binding protein-2. *J. Clin. Invest.* **101**: 2331–2339.
- Brown, M. S., and J. L. Goldstein. 1997. The SREBP pathway: regulation of cholesterol metabolism by proteolysis of a membrane-bound transcription factor. *Cell*. **89**: 331–340.
- Brown, M. S., and J. L. Goldstein. 1999. A proteolytic pathway that controls the cholesterol content of membranes, cells, and blood. *Proc. Natl. Acad. Sci. USA*. **96**: 11041–11048.
- Brown, M. S., J. Ye, R. B. Rawson, and J. L. Goldstein. 2000. Regulated intramembrane proteolysis: a control mechanism conserved from bacteria to humans. *Cell*. **100**: 391–398.
- Hua, X., C. Yokoyama, J. Wu, M. R. Briggs, M. S. Brown, J. L. Goldstein, and X. Wang. 1993. SREBP-2, a second basic-helix-loop-helix-leucine zipper protein that stimulates transcription by binding to a sterol regulatory element. *Proc. Natl. Acad. Sci. USA*. **90**: 11603–11607.
- Shimano, H., J. D. Horton, R. E. Hammer, I. Shimomura, M. S. Brown, and J. L. Goldstein. 1996. Overproduction of cholesterol and fatty acids causes massive liver enlargement in transgenic mice expressing truncated SREBP-1a. *J. Clin. Invest.* **98**: 1575–1584.
- Scharp, D. W., C. B. Kemp, M. J. Knight, W. F. Ballinger, and P. E. Lacy. 1973. The use of ficoll in the preparation of viable islets of langerhans from the rat pancreas. *Transplantation*. **16**: 686–689.
- Detimary, P., G. Van den Berghe, and J. C. Henquin. 1996. Concentration dependence and time course of the effects of glucose on adenine and guanine nucleotides in mouse pancreatic islets. *J. Biol. Chem.* **271**: 20559–20565.
- Folch, J., M. Lees, and G. H. Sloane Stanley. 1957. A simple method for the isolation and purification of total lipides from animal tissues. *J. Biol. Chem.* **226**: 497–509.
- Heider, J. G., and R. L. Boyett. 1978. The picomole determination of free and total cholesterol in cells in culture. *J. Lipid Res.* **19**: 514–518.
- Amemiya-Kudo, M., J. Oka, T. Ide, T. Matsuzaka, H. Sone, T. Yoshikawa, N. Yahagi, S. Ishibashi, J. Osuga, N. Yamada, et al. 2005. Sterol regulatory element-binding proteins activate insulin gene promoter directly and indirectly through synergy with BETA2/E47. *J. Biol. Chem.* **280**: 34577–34589.
- Hua, X., A. Nohturfft, J. L. Goldstein, and M. S. Brown. 1996. Sterol resistance in CHO cells traced to point mutation in SREBP cleavage-activating protein. *Cell*. **87**: 415–426.
- Dutta, S., S. Bonner-Weir, M. Montminy, and C. Wright. 1998. Regulatory factor linked to late-onset diabetes? *Nature*. **392**: 560.
- Kulkarni, R. N., U. S. Jhala, J. N. Winnay, S. Krajewski, M. Montminy, and C. R. Kahn. 2004. PDX-1 haploinsufficiency limits the compensatory islet hyperplasia that occurs in response to insulin resistance. *J. Clin. Invest.* **114**: 828–836.
- Fajas, L., J. S. Annicotte, S. Miard, D. Sarruf, M. Watanabe, and J. Auwerx. 2004. Impaired pancreatic growth, beta cell mass, and beta cell function in E2F1 (-/-) mice. *J. Clin. Invest.* **113**: 1288–1295.
- Ahlgren, U., J. Jonsson, and H. Edlund. 1996. The morphogenesis of the pancreatic mesenchyme is uncoupled from that of the pancreatic epithelium in IPF1/PDX1-deficient mice. *Development*. **122**: 1409–1416.
- Offield, M. F., T. L. Jetton, P. A. Labosky, M. Ray, R. W. Stein, M. A. Magnuson, B. L. Hogan, and C. V. Wright. 1996. PDX-1 is required for pancreatic outgrowth and differentiation of the rostral duodenum. *Development*. **122**: 983–995.
- Naya, F. J., H. P. Huang, Y. Qiu, H. Mutoh, F. J. DeMayo, A. B. Leiter, and M. J. Tsai. 1997. Diabetes, defective pancreatic morphogenesis, and abnormal enteroendocrine differentiation in BETA2/neuroD-deficient mice. *Genes Dev.* **11**: 2323–2334.
- Johnson, J. D., N. T. Ahmed, D. S. Luciani, Z. Han, H. Tran, J. Fujita, S. Mislis, H. Edlund, and K. S. Polonsky. 2003. Increased islet apoptosis in Pdx1 +/- mice. *J. Clin. Invest.* **111**: 1147–1160.
- Withers, D. J., J. S. Gutierrez, H. Towery, D. J. Burks, J. M. Ren, S. Previs, Y. Zhang, D. Bernal, S. Pons, G. I. Shulman, et al. 1998. Disruption of IRS-2 causes type 2 diabetes in mice. *Nature*. **391**: 900–904.
- Withers, D. J., D. J. Burks, H. H. Towery, S. L. Altamuro, C. L. Flint, and M. F. White. 1999. Irs-2 coordinates Igf-1 receptor-mediated beta-cell development and peripheral insulin signalling. *Nat. Genet.* **23**: 32–40.
- Kushner, J. A., J. Ye, M. Schubert, D. J. Burks, M. A. Dow, C. L. Flint, S. Dutta, C. V. Wright, M. R. Montminy, and M. F. White. 2002. Pdx1 restores beta cell function in Irs2 knockout mice. *J. Clin. Invest.* **109**: 1193–1201.

34. Zhang, C. Y., G. Baffy, P. Perret, S. Krauss, O. Peroni, D. Grujic, T. Hagen, A. J. Vidal-Puig, O. Boss, Y. B. Kim, et al. 2001. Uncoupling protein-2 negatively regulates insulin secretion and is a major link between obesity, beta cell dysfunction, and type 2 diabetes. *Cell*. **105**: 745–755.
35. Chan, C. B., D. De Leo, J. W. Joseph, T. S. McQuaid, X. F. Ha, F. Xu, R. G. Tsushima, P. S. Pennefather, A. M. Salapatek, and M. B. Wheeler. 2001. Increased uncoupling protein-2 levels in beta-cells are associated with impaired glucose-stimulated insulin secretion: mechanism of action. *Diabetes*. **50**: 1302–1310.
36. Lameloise, N., P. Muzzin, M. Prentki, and F. Assimacopoulos-Jeannet. 2001. Uncoupling protein 2: a possible link between fatty acid excess and impaired glucose-induced insulin secretion? *Diabetes*. **50**: 803–809.
37. Joseph, J. W., V. Koshkin, C. Y. Zhang, J. Wang, B. B. Lowell, C. B. Chan, and M. B. Wheeler. 2002. Uncoupling protein 2 knockout mice have enhanced insulin secretory capacity after a high-fat diet. *Diabetes*. **51**: 3211–3219.
38. Lee, Y., H. Hirose, M. Ohneda, J. H. Johnson, J. D. McGarry, and R. H. Unger. 1994. Beta-cell lipotoxicity in the pathogenesis of non-insulin-dependent diabetes mellitus of obese rats: impairment in adipocyte-beta-cell relationships. *Proc. Natl. Acad. Sci. USA*. **91**: 10878–10882.
39. Ishikawa, M., F. Okajima, N. Inoue, K. Motomura, T. Kato, A. Takahashi, S. Oikawa, N. Yamada, and H. Shimano. 2006. Distinct effects of pravastatin, atorvastatin, and simvastatin on insulin secretion from a beta-cell line, MIN6 cells. *J. Atheroscler. Thromb.* **13**: 329–335.
40. Brunham, L. R., J. K. Kruit, T. D. Pape, J. M. Timmins, A. Q. Reuwer, Z. Vasanji, B. J. Marsh, B. Rodrigues, J. D. Johnson, J. S. Parks, et al. 2007. Beta-cell ABCA1 influences insulin secretion, glucose homeostasis and response to thiazolidinedione treatment. *Nat. Med.* **13**: 340–347.
41. Brunham, L. R., J. K. Kruit, C. B. Verchere, and M. R. Hayden. 2008. Cholesterol in islet dysfunction and type 2 diabetes. *J. Clin. Invest.* **118**: 403–408.
42. Hao, M., W. S. Head, S. C. Gunawardana, A. H. Hasty, and D. W. Piston. 2007. Direct effect of cholesterol on insulin secretion: a novel mechanism for pancreatic beta-cell dysfunction. *Diabetes*. **56**: 2328–2338.